

Supplementary data

Speciation mapping of environmental samples using XANES imaging

Barbara E. Etschmann^{A,B}, Erica Donner^{C,D}, Joël Brugger^E, Daryl L. Howard^F, Martin D. de Jonge^F, David Paterson^F, Ravi Naidu^{C,D}, Kirk G. Scheckel^G, Chris G. Ryan^H and Enzo Lombi^{CI}

^AMineralogy, South Australian Museum, North Terrace, Adelaide, SA 5000, Australia.

^BSchool of Chemical Engineering, University of Adelaide, North Terrace, Adelaide, SA 5005, Australia.

^CCentre for Environmental Risk Assessment and Remediation, University of South Australia, Building X, Mawson Lakes Campus, SA 5095, Australia.

^DCRC CARE, PO Box 486, Salisbury, SA 5106, Australia.

^ESchool of Geosciences, Monash University, Clayton, Vic. 3800, Australia

^FAustralian Synchrotron, 800 Blackburn Road, Clayton, Vic. 3168, Australia

^GUS Environmental Protection Agency, Office of Research and Development, Cincinnati, OH, USA.

^HEarth Science and Resource Engineering, Commonwealth Scientific and Industrial Research Organisation (CSIRO), Clayton, Vic., Australia.

^ICorresponding author: enzo.lombi@unisa.edu.au

Fresh biosolid sample B3

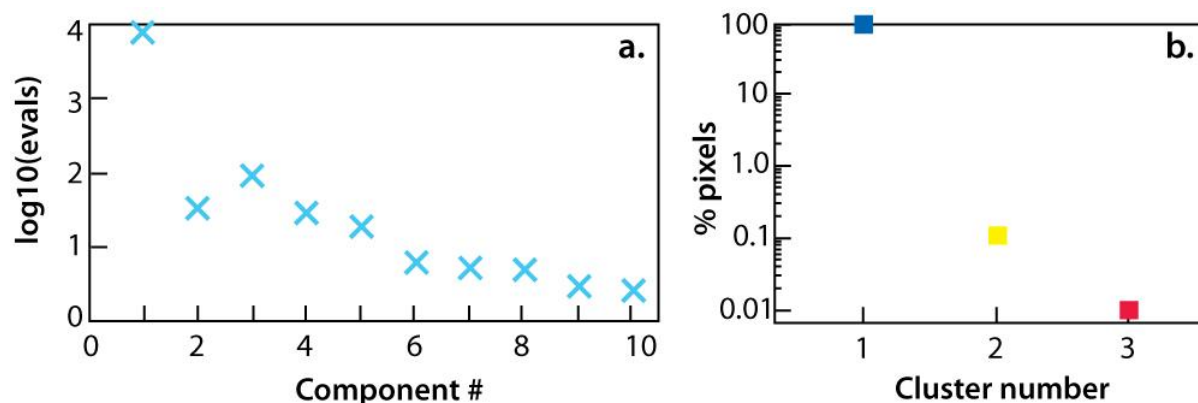


Fig. S1. Results of statistical analysis for sample B3. (a) log₁₀ eigenvalues determined by PCA. (b) percentage of pixels classified into cluster components. The components were switched manually and re-ordered in terms of their ‘interpretability’.

Table S1. Results of fits for selected individual pixels shown in Fig. 2

| | | |
|---|---|---|
| X = 215, y = 109, point #2 Red 76% Cu ₂ S + 24% Cu_HA $\chi^2_{\text{red}} = 0.81$ | X = 342, y = 100, point #1 Green 14% Cu ₂ S + 83% CuFe ₂ S ₃ + 3% Cu_HA $\chi^2_{\text{red}} = 0.20$ | X = 122, y = 35, point #3 Blue 7% Cu ₂ S + 25% CuFe ₂ S ₃ + 67% Cu_HA $\chi^2_{\text{red}} = 0.21$ |
| X = 83, y = 63, point #4 Red 67% Cu ₂ S + 33% Cu_HA $\chi^2_{\text{red}} = 0.48$ | X = 78, y = 60, point #5 Green 66% CuFe ₂ S ₃ + 34% Cu_HA $\chi^2_{\text{red}} = 2.00$ | X = 482, y = 54, point #6 Blue 21% CuFe ₂ S ₃ + 79% Cu_HA $\chi^2_{\text{red}} = 0.81$ |
| X = 365, y = 81, point #7 Red 100% Cu ₂ S $\chi^2_{\text{red}} = 1.95$ | X = 364, y = 76, point #8 Green 14% Cu ₂ S + 76% CuFe ₂ S ₃ + 10% Cu_HA $\chi^2_{\text{red}} = 0.77$ | X = 282, y = 13, point #9 Blue 13% CuFe ₂ S ₃ + 87% Cu_HA $\chi^2_{\text{red}} = 0.16$ |

Table S2. Results of fits for the XANES spectra shown in Fig. 3

| | | |
|---|---|---|
| High Cu:Fe ratio (magenta) 60% Cu ₂ S + 21% CuFe ₂ S ₃ + 19% CuHA $\chi^2_{\text{red}} = 0.29$ | Medium Cu:Fe ratio (green) 28% Cu ₂ S + 40% CuFe ₂ S ₃ + 32% CuHA $\chi^2_{\text{red}} = 0.03$ | Low Cu:Fe ratio (grey) 34% Cu ₂ S + 12% CuFe ₂ S ₃ + 53% CuHA $\chi^2_{\text{red}} = 0.21$ |
|---|---|---|

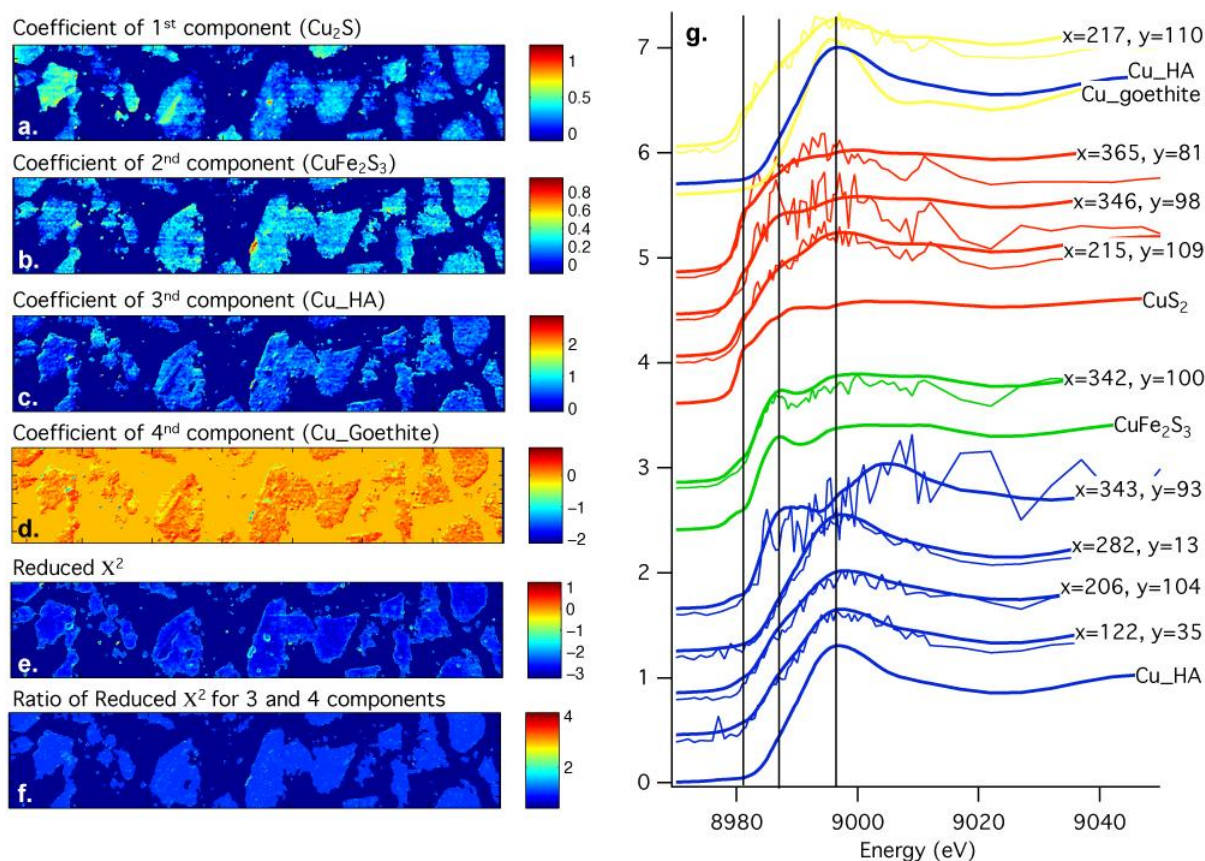


Fig. S2. Analysis of the XANES stack for sample B3 using a linear combination fit, using the dataset smoothed over 2×2 pixels. (a) Coefficient of 1st component (Cu₂S). (b) Coefficient of 2nd component (CuFe₂S₃). (c) Coefficient of 3rd component (Cu_HA). (d) Coefficient of 4th component (Cu_Goethite). (e) Map of the values of χ^2_{red} (log₁₀ scale). (f) Ratio of χ^2_{red} for the models containing 3 and 4 components, respectively. (g) Spectra at selected points.

Table S3. Results of fits for selected individual pixels shown in Fig. S2

| | | |
|--|--|--|
| X = 215, y = 109, point#2 yellow 52% Cu ₂ S + 28% CuFe ₂ S ₃ + 20% Cu_goethite $\chi^2_{\text{red}} = 0.77$ | X = 343, y = 93, point#1 Blue 54% CuFe ₂ S ₃ + 174% Cu_HA - 129% Cu_goethite $\chi^2_{\text{red}} = 4.00$ | X = 122, y = 35, point#3 Blue 9% Cu ₂ S + 22% CuFe ₂ S ₃ + 75% Cu_HA - 7% Cu_goethite $\chi^2_{\text{red}} = 0.21$ |
| X = 217, y = 110, point # yellow 50% Cu ₂ S + 21% CuFe ₂ S ₃ + 30% Cu_goethite $\chi^2_{\text{red}} = 0.62$ | X = 346, y = 98, point# Yellow 52% Cu ₂ S + 43% CuFe ₂ S ₃ + 5% Cu_goethite $\chi^2_{\text{red}} = 3.40$ | X = 342, y = 100, point # Blue 15% Cu ₂ S + 79% CuFe ₂ S ₃ + 5% Cu_goethite $\chi^2_{\text{red}} = 0.27$ |
| X = 365, y = 81, point# Red 94% Cu ₂ S + 6% Cu_goethite $\chi^2_{\text{red}} = 1.96$ | X = 206, y = 104, point # Blue 14% Cu ₂ S + 24% CuFe ₂ S ₃ + 82% Cu_HA - 20% Cu_goethite $\chi^2_{\text{red}} = 0.19$ | X = 282, y = 13, point # Blue 3% Cu ₂ S + 4% CuFe ₂ S ₃ + 110% Cu_HA - 17% Cu_goethite $\chi^2_{\text{red}} = 0.15$ |

Comparing 3 v. 4 components for B3

A further fit was conducted using four rather than three components, by including Cu^{II} sorbed on goethite as the fourth component (Figs 1k, S2). The Kelly et al.^[1] test was used to distinguish whether the two models were statistically significantly different

$$\frac{\chi^2_{\text{red},1}}{\chi^2_{\text{red},2}} - 1 \geq 2\sqrt{\frac{2}{\nu}}$$

where ν is the degrees of freedom. For XANES data, ν may be defined as the number of data points (80 in this instance, see HORAE_□ package^[2]) minus the number of variables used to fit the spectrum.

The sum of the matrix of χ^2_{red} for 3 components (C3) = 208, and for 4 components (C4) = 198, and C3/C4 ~1.07, which is not greater or equal to $1+2\times\sqrt{(2/80)} \sim 1.3$, implying that overall there is no statistically significant benefit in introducing a fourth component. Similarly, when the matrix of χ^2_{red} (3 components) was divided by the matrix of χ^2_{red} (4 components), most of the values were around one (Fig. S2f).

Aged biosolid sample B6

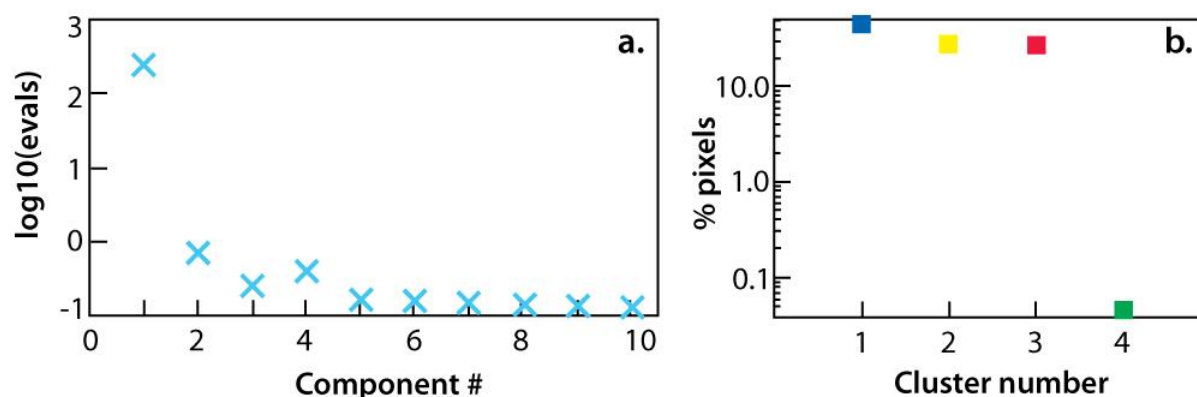


Fig. S3. Results of statistical analysis for sample B6. (a) log₁₀ eigenvalues determined by PCA. (b) percentage of pixels classified into cluster components. The components were switched manually and re-ordered in terms of their ‘interpretability’.

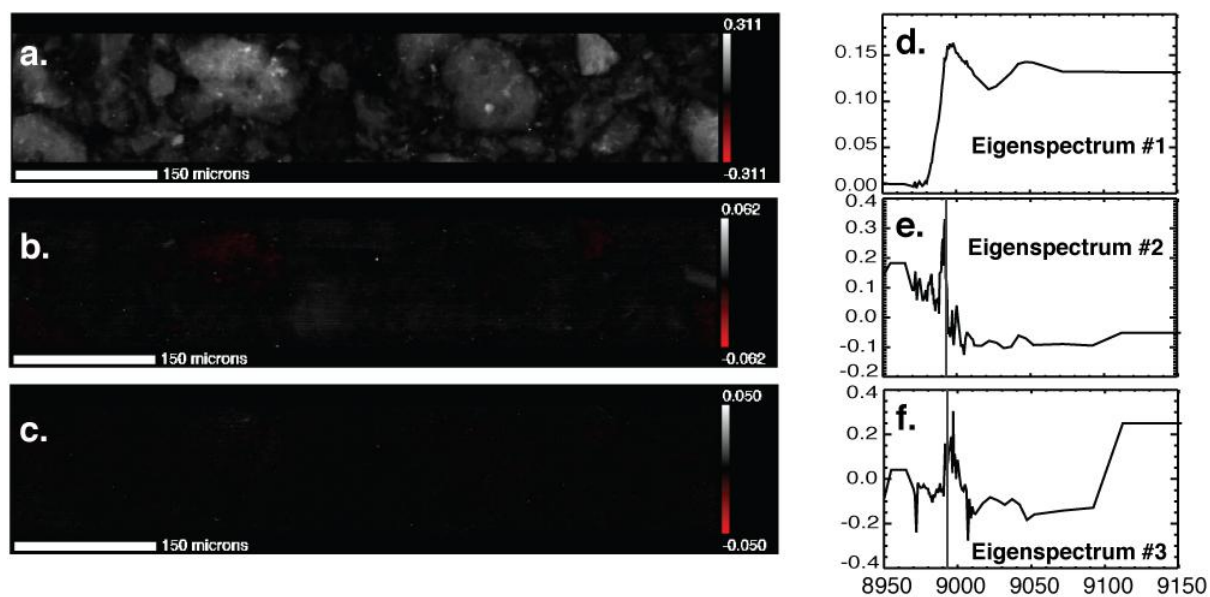


Fig. S4. Results of the ‘model-free’ analysis of the Cu K-edge XANES stack for sample B6. (a–c) Eigenimages and (d–f) corresponding eigenspectra.

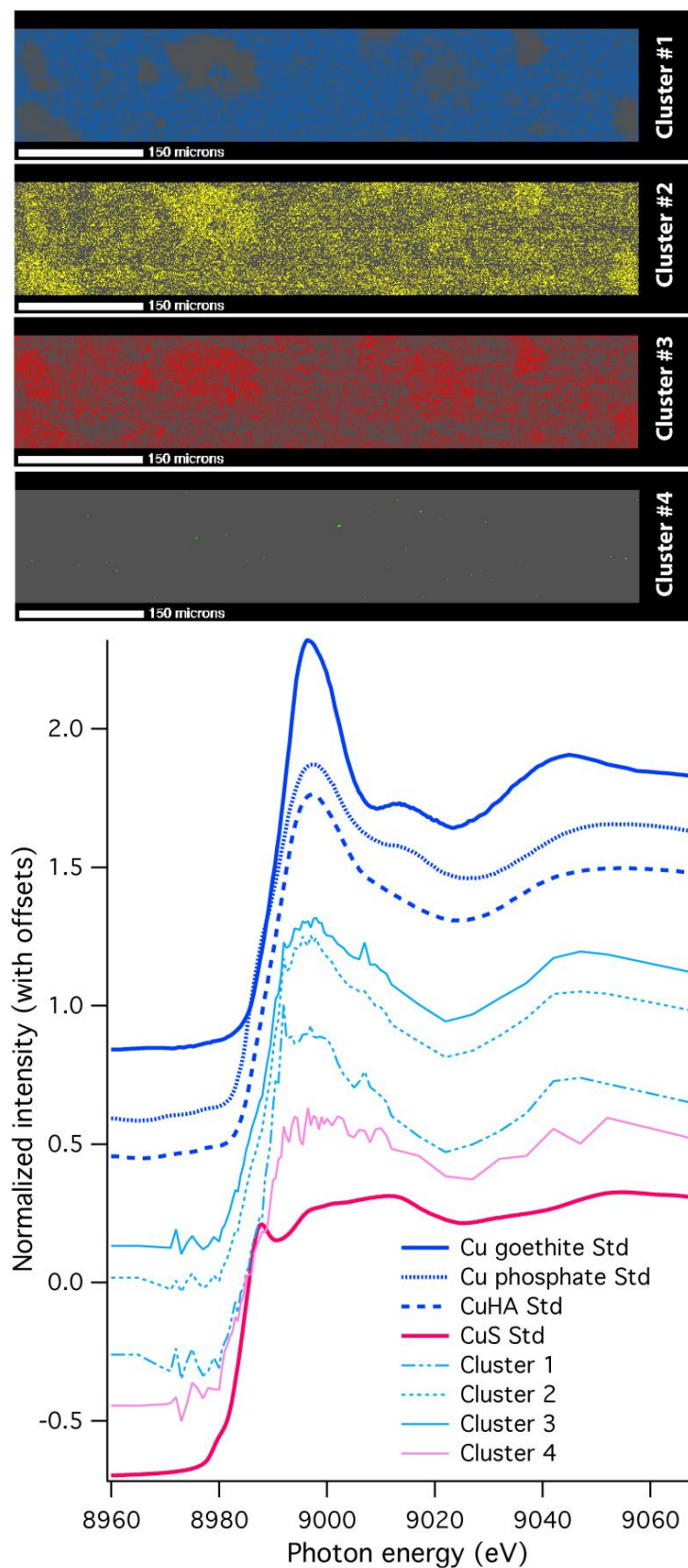


Fig. S5. Distribution and spectra of the four clusters. The spectra are compared to standards. Note that the signal quality does not allow to distinguish the Cu^{II} phosphate from Cu^{II} sorbed onto humic acid.

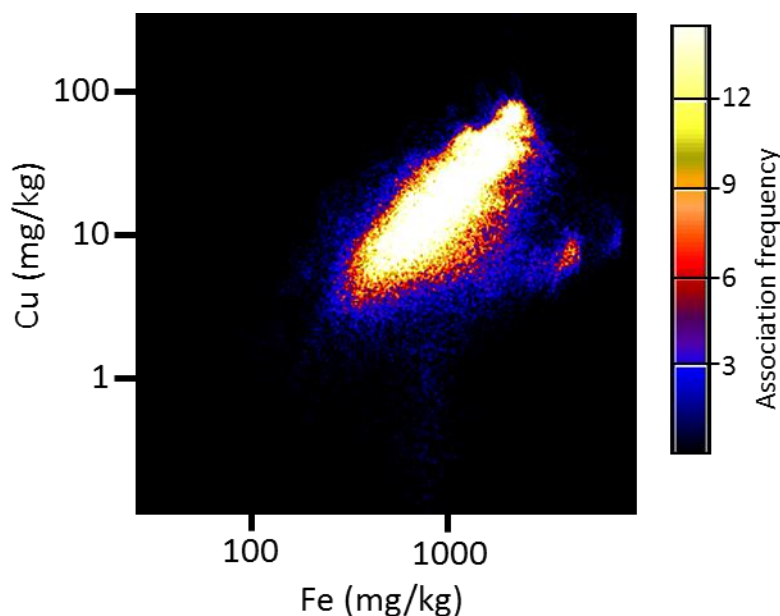


Fig. S6. Association plot showing the relationship between Cu and Fe concentrations for all data point collected in the elemental map of sample B6 (at 9152 eV).

Table S4. Results of fits for selected individual pixels shown in Fig. 4

| | | |
|---|---|---|
| X = 30, y = 25, point #1 Red 94% Cu_HA + 6% CuS $\chi^2_{\text{red}} = 0.32$ | X = 284, y = 1, point #4 Green 84% CuS + 18% Cu_goethite $\chi^2_{\text{red}} = 5.84$ | X = 216, y = 14, point #7 Blue 32% Cu_HA + 20% CuS + 48% Cu_goethite $\chi^2_{\text{red}} = 0.60$ |
| X = 235, y = 110, point #2 Red 85% Cu_HA + 15% CuS $\chi^2_{\text{red}} = 0.27$ | X = 486, y = 110, point #5 Green 45% Cu_HA + 55% CuS $\chi^2_{\text{red}} = 0.42$ | X = 242, y = 126, point #8 Blue 50% Cu_HA + 25% CuS + 25% Cu_goethite $\chi^2_{\text{red}} = 0.51$ |
| X = 737, y = 25, point #3 Red 86% Cu_HA + 14% CuS $\chi^2_{\text{red}} = 0.24$ | X = 548, y = 35, point #6 Green 4% Cu_HA + 89% CuS + 7% Cu_goethite $\chi^2_{\text{red}} = 0.52$ | X = 506, y = 61, point #9 Blue 34% Cu_HA + 39% CuS + 37% Cu_goethite $\chi^2_{\text{red}} = 0.39$ |

References

- [1] S. Kelly, D. Hesterberg, B. Ravel, Analysis of soils and minerals using X-ray absorption spectroscopy, in *Methods of Soil Analysis, Part 5. Mineralogical Methods* **2008**, Chapt. 14, pp. 387–463 (Soil Sciences Society of America: Madison, WI).
- [2] B. Ravel, M. Newville, ATHENA, ARTEMIS, HEPHAESTUS: data analysis for X-ray absorption spectroscopy using IFEFFIT. *J. Synchrotron Radiat.* **2005**, *12*, 537–541. [doi:10.1107/S0909049505012719](https://doi.org/10.1107/S0909049505012719)